



A high-throughput screening fluorescence polarization assay for fatty acid adenylating enzymes in *Mycobacterium tuberculosis*

Kimberly D. Grimes, Courtney C. Aldrich*

Center for Drug Design, University of Minnesota, 516 Delaware St. SE, Minneapolis, MN, USA

ARTICLE INFO

Article history:

Received 21 May 2011

Received in revised form 24 June 2011

Accepted 28 June 2011

Available online 2 July 2011

Keywords:

Mycobacterium tuberculosis

Adenylation

Adenylate-forming enzymes

Fluorescence polarization

High throughput screening

ABSTRACT

Mycobacterium tuberculosis, the etiological agent of tuberculosis (TB), encodes for an astonishing 34 fatty acid adenylating enzymes (FadDs), which play key roles in lipid metabolism. FadDs involved in lipid biosynthesis are functionally nonredundant and serve to link fatty acid and polyketide synthesis to produce some of the most architecturally complex natural lipids including the essential mycolic acids as well as the virulence-conferring phthiocerol dimycocerosates, phenolic glycolipids, and mycobactins. Here we describe the systematic development and optimization of a fluorescence polarization assay to identify small molecule inhibitors as potential antitubercular agents. We fluorescently labeled a bisubstrate inhibitor to generate a fluorescent probe/tracer, which bound with a K_D of 245 nM to FadD28. Next, we evaluated assay performance by competitive binding experiments with a series of known ligands and assessed the impact of control parameters including incubation time, stability of the signal, temperature, and DMSO concentration. As a final level of validation the LOPAC1280 library was screened in a 384-well plate format and the assay performed with a Z-factor of 0.75, demonstrating its readiness for high-throughput screening.

© 2011 Elsevier Inc. All rights reserved.

Tuberculosis (TB)¹ is an infectious disease caused by the acid-fast gram-positive bacillus *Mycobacterium tuberculosis* (*Mtb*) that is readily spread by aerosolized droplets from coughing or sneezing of an actively infected individual [1]. Improvements in public health and ultimately the discovery of effective chemotherapeutic agents in the middle of last century led to a drastic reduction of TB mortality in the industrialized world. However, TB has continued to rage in the developing world and now infects approximately 2 billion individuals resulting in nearly two million deaths annually, making TB the second leading cause of infectious disease mortality superseded only by HIV/AIDS [1]. The emergence of multidrug resistant (MDR-TB) strains, and more recently, extensively drug resistant (XDR-TB) strains that are virtually untreatable, demands the development of new TB drugs.

* Corresponding author. Fax: +1 612 626 8154.

E-mail address: aldri015@umn.edu (C.C. Aldrich).

¹ Abbreviations used: ACP, acyl carrier protein; Boc, *tert*-butoxycarbonyl; DME, 1,2-dimethoxyethane; DMF, *N,N*-dimethylformamide; FAAL, fatty acyl-AMP ligase; FACL, fatty acyl CoA ligase; FadD, fatty acid adenylating enzyme; FP, fluorescence polarization; HTS, high-throughput screening; ITC, isothermal titration calorimetry; MBT, mycobactin; MDR-TB, multidrug resistant tuberculosis; MesG, 7-methylthioguanosine; *Mtb*, *Mycobacterium tuberculosis*; NHS, *N*-hydroxylsuccinimidyl; PDIM, phthiocerol dimycocerosate; PGL, phenolic glycolipid; PKS, polyketide synthase; pTsOH, *p*-toluenesulfonic acid; SL, sulfolipid; TAMRA, 5-carboxytetramethylrhodamine; TB, tuberculosis; TCEP, tris(2-carboxyethyl)phosphine; TFA, trifluoroacetic acid; XDR-TB, extensively drug resistant tuberculosis.

Mycobacteria contain a unique cell envelope, composed of many novel lipids, which provides a permeability barrier that shields the bacterium from environmental stress, provides intrinsic resistance to chemotherapeutic agents, and plays a key role in persistence [2–5]. Lipids in the mycobacterial envelope include the covalently attached mycolic acids that are essential as well as several noncovalently associated lipids such as the phthiocerol dimycocerosates (PDIMs), phenolic glycolipids (PGLs), sulfolipids (SLs), and mycobactins (MBTs) that are critical for virulence (Fig. 1) [6–9]. Fatty acid degradation in mycobacteria is also believed to be important and several lines of evidence support the hypothesis that mycobacteria are primarily lipolytic *in vivo*, deriving their nutrients by breakdown of host fatty acids [10,11].

The FadD enzymes are found in both lipid biosynthetic as well as catabolic pathways [12]. *M. tuberculosis* encodes for an astonishing 34 *fadDs*, by comparison, *Escherichia coli* encodes a single *fadD* [13]. The large number of *fadDs* found in *Mtb* highlights the importance of lipid metabolism in this organism. FadDs catalyze a two-step reaction. In the first step, the FadD binds a substrate alkanolic acid and ATP, and then catalyzes their condensation to form an intermediate acyl-adenylate with the release of pyrophosphate. In a second step, the FadD binds an acceptor molecule, which can be either a molecule of coenzyme A (CoA) or an acyl carrier protein (ACP) domain of a polyketide synthase (PKS) enzyme, then catalyzes the transfer of the acyl moiety of the acyl-adenylate onto

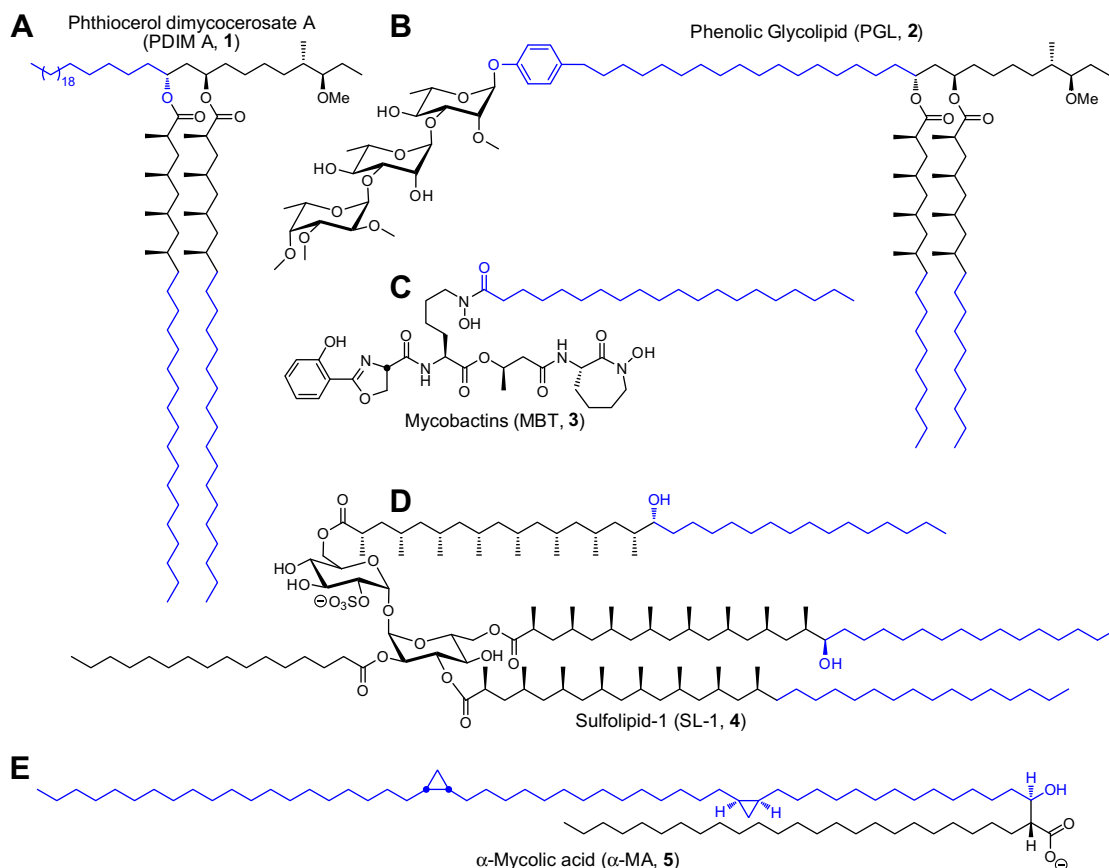


Fig. 1. Unique lipids found in the *Mycobacterium tuberculosis* cell envelope. The *FadD*s are involved in the biosynthesis of the lipid portions in each of these molecules as highlighted in blue. (A) Phthiocerol dimycocerosate A (PDIM A, **1**) biosynthesis requires *FadD26* and *FadD28*; (B) phenolic glycolipids (PGLs, **2**) require *FadD22*, *FadD28*, and *FadD29*; (C) the mycobactins (MBTs, **3**) utilize *FadD33*; (D) sulfolipids, represented by SL-1 **4**, require *FadD23*; and (E) the mycolic acids, represented α -mycolic acid (α -MA, **5**), employ *FadD32*.

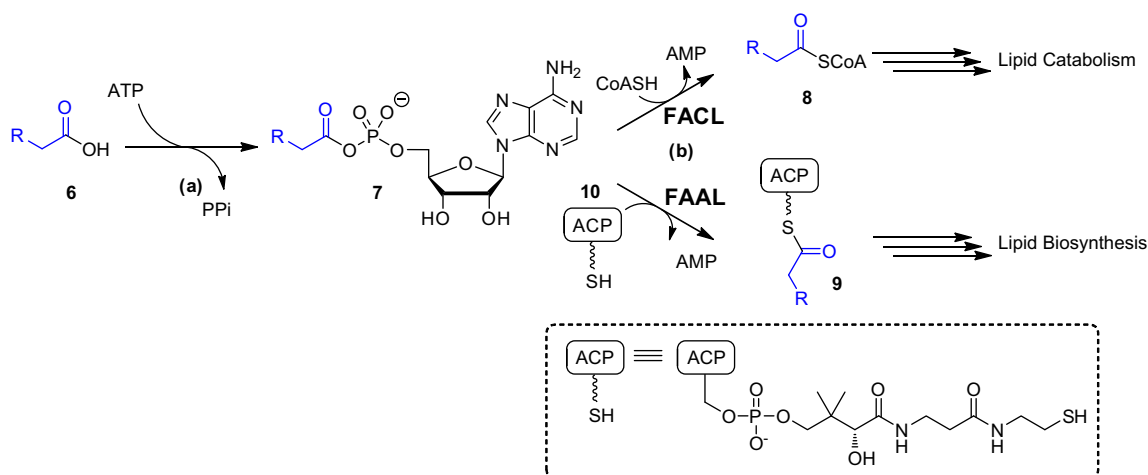


Fig. 2. Mechanism of fatty acid adenylating enzymes (*FadD*s) in *Mycobacterium tuberculosis*. *FadD*s catalyze a two-step reaction: (a) the first half-reactions of both *FAcL* and *FAAL* classes of *FadD* are identical and involve the formation of an acyl-adenylate intermediate **7** from a fatty acid **6** and ATP with the release of pyrophosphate; (b) the second half-reaction for the *FAcL* and *FAAL* classes of *FadD* diverges and involves the transfer of the acyl group of the acyl-adenylate **7** onto the nucleophilic thiol of CoA for *FAcL*s, the first step in lipid catabolism or the thiolation domain of an acyl carrier protein (ACP), which is the first step in fatty acid biosynthesis.

the nucleophilic sulfur atom of the acceptor molecule resulting in a CoA thioester or an acylated-ACP product (Fig. 2) [12,14].

As a result of this functional dichotomy, the *FadD*s in *Mtb* are grouped into two classes: fatty acyl-CoA ligases (*FAcL*s) involved in fatty acid catabolism and long chain fatty acyl-AMP ligases

(*FAAL*s) involved in fatty acid biosynthesis [12]. The precise biochemical roles of the 20 annotated *FAcL*s are largely unknown: *FadD6*, *FadD13*, *FadD15*, *FadD17*, and *FadD19* have been biochemically characterized as CoA ligases, but the native substrates for these enzymes have not been identified [12,15,16]. Transposon

mutagenesis suggested the FAALs were nonessential, which may be due to functional redundancy [17]. Indeed FadD6, FadD15, and FadD19 were shown to possess a remarkably broad substrate specificity [15]. By contrast, the FAAL class of FadDs appears to be functionally nonredundant and serves to link fatty acid and polyketide synthesis in mycobacteria [12,18]. FadD32, for example, is required for mycolic acid biosynthesis and targeted genetic disruption confirmed its essentiality [19–21]. FadD33 is responsible for attachment of the lipid moiety onto the mycobactins [22–24]. FadD26 and FadD28 are required for synthesis of the phthiocerol and mycocerosic acids in the PDIMs [25–27]. FadD22 in conjunction with FadD29 is required for assembly of the phenolphthiocerol lipid in the PGLs [27,28]. The sulfolipids use FadD23 for biosynthesis of the phthioceranic acid and two hydroxyphthioceranic acid groups [29].

The identification of specific small molecule inhibitors against each class of FadDs or selective inhibitors of an individual FadD is expected to help decipher the functional role that the FadDs play in lipid metabolism and could additionally lead to the development of a new class of antitubercular agents. Simple bisubstrate inhibitors of the FadDs have been described that serve as useful tool compounds, but these inhibitors possess only modest potency, display little selectivity, and do not represent useful drug-like leads [14,21]. High-throughput screening represents an alternate method for identifying potential lead compounds with more chemically tractable scaffolds.

We recently reported the development of a coupled steady-state kinetic assay for FadDs employing hydroxylamine as a surrogate acceptor molecule, which led to hydroxamate products [30]. The pyrophosphate generated in the first half-reaction catalyzed by the FadD was measured using pyrophosphatase and purine nucleoside phosphorylase in conjunction with the chromogenic product 7-methylthioguanosine (MesG). While this assay represents an excellent functional assay for secondary screening, it is not suitable for HTS due to the requirement for two coupling enzymes, potential interference caused by the low wavelength of detection, and low activity of most FadDs. Instead, we elected to design a fluorescent polarization (FP) displacement assay to identify active-site-directed FadD inhibitors.

Fluorescence polarization assays have been widely used for high-throughput screening due to their operational simplicity and robust performance [31–33]. FP displacement assays involve displacement of a fluorescently labeled ligand, also referred to as a tracer, by a small molecule from a macromolecular receptor, which is usually a protein. The degree of polarization of the fluorescent ligand is related to its rotational correlation time and hence molecular mass. When a fluorescent ligand is bound to a high molecular weight receptor such as a protein, it tumbles slowly and the emitted light remains largely polarized. However, when a fluorescent ligand is displaced into solution, by a competitive ligand, the fluorescent ligand tumbles rapidly and the emitted light is depolarized. For analysis of ligand dissociation constants, anisotropy is more convenient to use than polarization values; consequently we will use anisotropy for data analysis rather than polarization in the FP assay [33].

Herein, we describe the development of a fluorescence polarization displacement assay for the discovery of inhibitors of the FAAL class of FadDs. We selected FadD28 as a model FadD since this enzyme is required for biosynthesis of the virulence conferring PDIM and DIM lipids, FadD28 can be readily overexpressed and purified from *E. coli*, and FadD28 is the only FadD from *Mtb* that has been structurally characterized [14,34]. We first prepared a fluorescently labeled active-site-directed FP probe that exhibited nanomolar affinity for FadD28. We then performed competitive displacement experiments with a series of known ligands of varying potency to validate the assay. Next, we examined the impact of

assay parameters including incubation time, temperature, and DMSO concentration. The performance of the assay was then evaluated in a 384-well plate format against the LOPAC1280 library.

Materials and methods

General methods, reagents, procedures

All commercial reagents (Sigma–Aldrich, Fisher, Fluka) were used as provided. 5-Carboxytetramethylrhodamine *N*-hydroxysuccinimide ester was obtained from Berry & Associates (Dexter, MI). Dichlorobis(triphenylphosphine)palladium (II) and copper iodide were purchased from Strem Chemicals (Newburyport, MA). Sulfamoyl chloride was prepared by the method of Heacock without recrystallization [35]. 2-Iodoadenosine **12** was prepared in three steps from guanosine using the method of Matsuda et al. [36]. *tert*-Butyl 2-(2-(2-hydroxyethoxy)ethoxy)ethylcarbamate was synthesized in two steps from commercially available 2-[2-(2-chloroethoxy)ethoxy]ethanol [37,38]. An anhydrous solvent dispensing system (J.C. Meyer) using two packed columns of neutral alumina was used for drying *N,N*-dimethylformamide (DMF) and the solvent was dispensed under Argon. Anhydrous dimethoxyethane (DME) and acetonitrile (MeCN) were used as provided. All reactions were performed under an inert atmosphere of dry argon in oven-dried (150 °C) glassware. Flash chromatography was performed on an ISCO Combiflash Companion purification system with prepacked silica gel cartridges and the indicated solvent system. ¹H and ¹³C NMR experiments were recorded on a Varian 600 MHz spectrometer. Proton chemical shifts are reported in ppm from an internal standard of residual methanol (3.31 ppm) or chloroform (7.21 ppm). Carbon chemical shifts are reported using an internal standard of residual methanol (49.1 ppm) or chloroform (77.2 ppm). Proton chemical data are reported as follows: chemical shift, multiplicity (s = singlet, d = doublet, t = triplet, q = quartet, p = pentet, m = multiplet, br = broad, ovlp = overlapping), coupling constant, and integration. ¹³C NMR data for probe **11** were obtained by HSQC and HMBC experiments. High-resolution mass spectra were acquired on an Agilent TOF II TOF/MS instrument equipped with an ESI or APCI interface. Semi-preparative HPLC was performed on a Phenomenex Gemini 10 μm C18 110A (250 × 10.0 mm) column operating at 4.0 mL/min with detection at 254 nm.

Cloning, expression, and purification of FadD28

FadD28 was cloned, overproduced, and purified as previously reported to afford approximately 90 mg/L of culture [30].

Synthesis of fluorescent probe **11**

tert-Butyl 2-[2-[2-(prop-2-yn-1-yloxy)ethoxy]ethoxy]ethylcarbamate (**13**): to a solution of *tert*-butyl 2-[2-(2-hydroxyethoxy)ethoxy]ethylcarbamate (920 mg, 3.69 mmol, 1.0 eq) in THF (40 mL) was added sodium hydride (60% dispersion in oil, 221 mg, 5.54 mmol, 1.5 eq) in one portion at 0 °C. After 0.5 h, propargyl bromide (80% in toluene, 411 μL, 3.69 mmol, 1.0 eq) was added and the reaction mixture was warmed to 23 °C and stirred for 16 h. The reaction was quenched with saturated aqueous NH₄Cl (10 mL) and extracted with EtOAc (3 × 25 mL). The combined extracts were washed with saturated aqueous NaCl (50 mL), dried (MgSO₄), and concentrated. Purification by flash chromatography (0–50% hexanes/EtOAc) afforded the title compound (525 mg, 50%) as a colorless oil: *R*_f 0.62 (3:2 EtOAc/hexane); ¹H NMR (600 MHz, CDCl₃): δ 1.45 (s, 9H), 2.44 (t, *J* = 2.4 Hz, 1H), 3.32–3.33 (m, 2H), 3.55 (t, *J* = 4.8 Hz, 2H), 3.63–3.64 (m, 2H), 3.65–3.67

(m, 2H), 3.69–3.70 (m, 2H), 3.72–3.73 (m, 2H), 4.23 (d, $J = 2.4$ Hz, 2H), 5.03 (br s, 1H); ^{13}C NMR (150 MHz, CDCl_3): δ 28.3, 40.3, 58.3, 68.9, 70.08, 70.13, 70.3, 70.4, 74.7, 78.9, 79.5, 155.9; HRMS (APCI+) calcd for $\text{C}_{14}\text{H}_{26}\text{NO}_5$ $[\text{M}+\text{H}]^+$ 288.1805, found 288.1788 (error 5.9 ppm).

2-[3-(2-{2-[2-(*tert*-Butoxycarbonylamino)ethoxy]ethoxy}ethoxy)prop-1-ynyl]adenosine (**14**): compound **13** (431 mg, 1.5 mmol, 3.0 eq) was added dropwise via a syringe pump over 0.5 h to a solution of 2-iodoadenosine **12** (197 mg, 0.5 mmol, 1.0 eq), dichlorobis(triphenylphosphine)palladium (II) (17.5 mg, 0.025 mmol, 0.05 eq), and copper iodide (7.1 mg, 0.038 mmol, 0.076 eq) in $\text{CH}_3\text{CN}/\text{Et}_3\text{N}$ (1:1 v/v, 10 mL). The reaction was stirred 3 h at 23 °C, and then concentrated *in vacuo*. Purification by flash chromatography (0–10% EtOAc/MeOH) afforded the title compound (260 mg, 94%) as a yellow oil: R_f 0.3 (8:2 EtOAc/MeOH); ^1H NMR (600 MHz, CD_3OD) δ 1.42 (s, 9H), 3.21–3.23 (m, 2H), 3.51 (t, $J = 6.0$ Hz, 2H), 3.61–3.63 (m, 2H), 3.65–3.67 (m, 2H) 3.70–3.72 (m, 2H), 3.75 (dd, $J = 12.0$, 2.4 Hz, 1H), 3.79–3.80 (m, 2H), 3.90 (dd, $J = 12.6$, 2.4 Hz, 1H), 4.17 (q, $J = 2.4$ Hz, 1H), 4.33 (dd, $J = 5.4$, 3.0 Hz, 1H), 4.45 (s, 2H), 4.71 (t, $J = 6.0$ Hz, 1H), 5.94 (d, $J = 6.0$ Hz, 1H), 6.58 (br s, 1H), 8.34 (s, 1H); ^{13}C NMR (150 MHz, CD_3OD) δ 28.9, 41.4, 58.5, 63.5, 70.5, 71.2, 71.3, 71.5, 71.6, 72.6, 75.6, 80.2, 83.2, 85.9, 88.1, 91.3, 120.7, 142.9, 146.8, 150.2, 157.4, 158.5; HRMS (ESI–) calcd for $\text{C}_{24}\text{H}_{35}\text{N}_6\text{O}_9$ $[\text{M}-\text{H}]^-$ 551.2471, found 551.2480 (error 1.6 ppm).

2-[3-(2-{2-[2-(*tert*-Butoxycarbonylamino)ethoxy]ethoxy}ethoxy)prop-1-ynyl]-2',3'-*O*-isopropylideneadenosine (**15**): to a solution of **14** (125 mg, 0.23 mmol, 1.0 eq) in acetone (5 mL) was added dimethoxypropane (139 μL , 1.13 mmol, 4.9 eq) and *p*-toluenesulfonic acid (88 mg, 0.25 mmol, 1.09 eq). The reaction was stirred at 23 °C for 16 h. To the resulting suspension was added solid NaHCO_3 to quench the reaction and then the acetone was removed *in vacuo*. The residue was partitioned between EtOAc (20 mL) and saturated aqueous NaHCO_3 . The aqueous layer was further extracted with EtOAc (3 \times 20 mL). The combined extracts were washed with saturated aqueous NaCl (50 mL), dried (MgSO_4), and concentrated. Purification by flash chromatography (0–10% $\text{CH}_2\text{Cl}_2/\text{MeOH}$) afforded the title compound (120 mg, 88%) as a yellow oil: R_f 0.5 (9:1 $\text{CH}_2\text{Cl}_2/\text{MeOH}$); ^1H NMR (600 MHz, CD_3OD) δ 1.39 (s, 3H), 1.42 (s, 9H), 1.62 (s, 3H), 3.22 (t, $J = 5.4$ Hz, 2H), 3.51 (t, $J = 6.0$ Hz, 2H), 3.61–3.63 (m, 2H), 3.65–3.67 (m, 2H) 3.70–3.74 (m, 3H), 3.79–3.81 (m, 3H), 4.37 (q, $J = 3.6$ Hz, 1H), 4.46 (s, 2H), 5.04 (dd, $J = 6.0$, 3.0 Hz, 1H), 5.25 (dd, $J = 6.0$, 3.0 Hz, 1H), 6.14 (d, $J = 3.6$ Hz, 1H), 8.36 (s, 1H); ^{13}C NMR (150 MHz, CD_3OD) δ 25.8, 27.8, 28.9, 41.5, 59.6, 63.8, 70.6, 71.2, 71.4, 71.6, 71.7, 80.1, 83.0, 83.1, 85.5, 86.2, 88.3, 92.9, 115.4, 120.3, 142.8, 147.2, 150.3, 157.3, 158.5; HRMS (ESI–) calcd for $\text{C}_{27}\text{H}_{39}\text{N}_6\text{O}_9$ $[\text{M}-\text{H}]^-$ 591.2784, found 591.2787 (error 0.5 ppm).

2-[3-(2-{2-[2-(*tert*-Butoxycarbonylamino)ethoxy]ethoxy}ethoxy)prop-1-ynyl]-2',3'-*O*-isopropylidene-5'-*O*-(sulfamoyl)adenosine (**16**): to a solution of **15** (70 mg, 0.12 mmol, 1.0 eq) in DME (10 mL) was added sodium hydride (60% dispersion in mineral oil, 13.0 mg, 0.33 mmol, 2.75 eq) at 0 °C. After 0.5 h, solid sulfamoyl chloride (20.4 mg, 0.18 mmol) was added and the reaction was stirred for 1 h at 23 °C. The mixture was quenched with MeOH (5 mL), and then concentrated onto Celite. Purified by flash chromatography (0–20% EtOAc/MeOH) afforded the title compound (50 mg, 62%) as a yellow oil: R_f 0.75 (8:2 EtOAc/MeOH); ^1H NMR (600 MHz, CD_3OD) δ 1.40 (s, 3H), 1.42 (s, 9H), 1.62 (s, 3H), 3.22 (t, $J = 5.4$ Hz, 2H), 3.52 (t, $J = 5.4$ Hz, 2H), 3.61–3.62 (m, 2H), 3.65–3.66 (m, 2H) 3.71–3.72 (m, 2H) 3.79–3.80 (m, 2H), 4.28 (dd, $J = 10.8$, 4.8 Hz, 1H), 4.38 (dd, $J = 10.5$, 4.2 Hz, 1H), 4.48 (s, 2H), 4.53 (q, $J = 4.8$ Hz, 1H), 5.14 (dd, $J = 5.4$, 3.0 Hz, 1H), 5.39 (dd, $J = 6.0$, 3.0 Hz, 1H), 6.14 (d, $J = 2.4$ Hz, 1H), 8.23 (s, 1H); ^{13}C NMR (150 MHz, CD_3OD) δ 25.8, 27.6, 28.9, 41.4, 59.6, 70.1, 70.7, 71.2, 71.4, 71.5, 71.7, 80.2, 83.2, 83.8, 85.6, 85.7, 86.1, 92.0,

115.8, 120.3, 142.8, 146.3, 150.3, 156.8, 158.5; HRMS (ESI–) calcd for $\text{C}_{27}\text{H}_{40}\text{N}_7\text{O}_{11}\text{S}$ $[\text{M}-\text{H}]^-$ 670.2512, found 670.2533 (error 3.1 ppm).

2-[3-(2-{2-[2-(*tert*-Butoxycarbonylamino)ethoxy]ethoxy}ethoxy)prop-1-ynyl]-2',3'-*O*-isopropylidene-5'-*O*-[*N*-(*n*-tetradecanoyl)sulfamoyl]adenosine triethylammonium salt (**18**): To a solution of **16** (40 mg, 0.06 mmol, 1.0 eq) in DMF (5 mL) at 0 °C was added *N*-hydroxysuccinimidyl tetradecanoate **17** (29 mg, 0.09 mmol, 1.5 eq) and Cs_2CO_3 (58 mg, 0.18 mmol, 3.0 eq). The reaction was stirred for 16 h at 23 °C and then filtered to remove salts and the filtrate was concentrated. Purification by flash chromatography (90:10:0.5 EtOAc/MeOH/ NEt_3) afforded the title compound (45 mg, 77%) as a yellow oil: R_f 0.4 (9:1 EtOAc/MeOH); ^1H NMR (600 MHz, CD_3OD) δ 0.89 (t, $J = 6.6$ Hz, 3H), 1.25–1.31 (m, 29H), 1.39 (s, 3H), 1.42 (s, 9H), 1.56 (p, $J = 7.2$ Hz, 2H), 1.62 (s, 3H), 2.17 (t, $J = 7.2$ Hz, 2H), 3.18–3.23 (m, 8H), 3.51 (t, $J = 5.4$ Hz, 2H), 3.61–3.62 (m, 2H), 3.66–3.67 (m, 2H), 3.71–3.72 (m, 2H), 3.79–3.81 (m, 2H), 4.23–4.28 (m, 2H), 4.46 (s, 2H), 4.53 (br s, 1H), 5.10 (dd, $J = 5.7$, 1.8 Hz, 1H), 5.30 (dd, $J = 6.0$, 3.0 Hz, 1H), 6.22 (d, $J = 3.0$ Hz, 1H), 8.50 (s, 1H); ^{13}C NMR (150 MHz, CD_3OD) δ 9.3, 14.6, 23.8, 25.8, 27.5, 27.7, 28.9, 30.4, 30.58, 30.63, 30.69, 30.74, 30.81, 30.87, 30.88, 33.2, 40.3, 41.4, 47.9, 59.6, 69.9, 70.6, 71.2, 71.4, 71.5, 71.6, 80.1, 82.7, 83.3, 85.8, 85.9, 86.5, 91.6, 115.5, 119.8, 142.3, 147.3, 150.8, 157.2, 158.5, 182.9; HRMS (ESI–) calcd for $\text{C}_{41}\text{H}_{66}\text{N}_7\text{O}_{12}\text{S}$ $[\text{M}-\text{H}]^-$ 880.4496, found 880.4496 (error 0 ppm).

2-[3-(2-{2-[2-({4-Carboxy-3-[6-(dimethylamino)-3-(dimethyliminio)-3*H*-xanthen-9-yl]benzoyl]amino)ethoxy]ethoxy}ethoxy)prop-1-ynyl]-5'-*O*-[*N*-(*n*-tetradecanoyl)sulfamoyl]adenosine triethylammonium salt (**11**): to **18** (10 mg, 0.01 mmol, 1.0 eq) was added 80% TFA (1.5 mL). The reaction was stirred at 23 °C for 4 h, and then concentrated *in vacuo* to remove all traces of TFA. The residue was dissolved in DMF (350 μL) and triethylamine (6.0 μL , 0.045 mmol, 4.5 eq) and 5-carboxytetramethylrhodamine *N*-hydroxysuccinimide ester **19** (TAMRA, 8.0 mg, 0.015 mmol, 1.5 eq) were added. The flask was covered with foil and the mixture was stirred at 23 °C for 5 h. The mixture was directly purified by semipreparative HPLC (injected 5 \times 70 μL) using a Phenomenex Gemini 10 μm C18 110A (250 \times 10.0 mm) column and a linear gradient of 20–100% $\text{CH}_3\text{CN}/50$ mM triethylammonium bicarbonate (pH 7.5) over 15 min followed by 100% CH_3CN for 10 min. The retention time of the product was 19.0 min and the appropriate fractions were pooled and lyophilized to afford the title compound (6.0 mg, 48%) as a magenta solid: ^1H NMR (600 MHz, CD_3OD) δ 0.89 (t, $J = 7.2$ Hz, 3H), 1.25–1.31 (m, 29H), 1.60 (p, $J = 7.2$ Hz, 2H), 2.20 (t, $J = 7.8$ Hz, 2H), 3.19 (q, $J = 7.8$ Hz, 6H), 3.25 (s, 6H), 3.27 (s, 6H), 3.67–3.68 (m, 4H), 3.69–3.70 (m, 6H), 3.74 (t, $J = 5.4$ Hz, 2H), 4.16–4.17 (m, 1H), 4.25–4.34 (ovlp m, 3H), 4.30 (ovlp s, 2H), 4.43 (t, $J = 4.8$ Hz, 1H), 5.84 (d, $J = 5.4$ Hz, 1H), 6.74 (br s, 2H), 6.87 (d, $J = 9.0$ Hz, 1H), 6.92 (d, $J = 9.0$ Hz, 1H), 7.16 (d, $J = 9.6$ Hz, 1H), 7.19 (d, $J = 9.0$ Hz, 1H), 7.69 (d, $J = 7.2$ Hz, 1H), 8.12 (d, $J = 7.8$ Hz, 1H), 8.49 (s, 1H), 8.54 (s, 1H); ^{13}C NMR (150 MHz, CD_3OD) δ 9.5, 14.6, 23.9, 27.7, 30.3 (3C), 30.6, 30.8 (2C), 30.9 (2C), 33.2, 40.5, 41.0 (2C), 41.1 (2C), 41.2, 48.0, 59.6, 68.8, 70.5, 70.8, 71.7 (2C), 71.9, 72.0, 76.4, 79.6, 83.7, 84.4, 89.3, 96.9 (2C), 114.5 (2C), 114.9 (2C), 119.6, 128.9, 129.8, 131.5, 132.4 (2C), 136.9, 138.8, 142.1, 147.6, 155.5, 158.6, 162.1, 162.3 (2C), 166.4, 169.2, 172.4, 180.1 (missing C2 and C6 of the adenine ring, for complete assignment by COSY, HMQC, and HMBC, see Supplementary data); HRMS (ESI–) calcd for $\text{C}_{58}\text{H}_{74}\text{N}_9\text{O}_{14}\text{S}$ $[\text{M}-\text{H}]^-$ 1152.5081, found 1152.5014 (error 5.8 ppm).

Equilibrium dissociation constant of probe **11**

Direct binding experiments were performed to determine the equilibrium dissociation constant (K_D) between FP probe **11** and Fadd28. Threefold serial dilutions of a 3 \times stock solution of Fadd28

(10 μL , 75 μM) in $1\times$ FP buffer (30 mM Trizma-HCl, pH 7.5, 1 mM MgCl_2 , 1 mM TCEP, 0.0025% Igepal CA-630) were added to 20 μL of a 1.5X stock solution of **11** (150 nM) in $1\times$ FP buffer in a 384-well black plate (Corning No. 3575). The plate was shaken for 5 s and read ($\lambda_{\text{ex}} = 530$, $\lambda_{\text{em}} = 590$, emission cutoff = 590 nm, G factor = 1.104) after a 10 min incubation period at 23 $^\circ\text{C}$ on a Molecular Devices Spectramax M5e plate reader. The K_D was determined by fitting the experimentally observed anisotropies (A_{OBS}) to Eqs. (1) and (2) by nonlinear regression analysis using Mathematica 7 (Wolfram Research Inc.):

$$A_{\text{OBS}} = \frac{QF_{\text{SB}}A_B + (1 - F_{\text{SB}})A_F}{1 - (1 - Q)F_{\text{SB}}} \quad (1)$$

$$F_{\text{SB}} = \frac{K_{D1} + L_{\text{ST}} + R_T - \sqrt{(K_{D1} + L_{\text{ST}} + R_T)^2 - 4L_{\text{ST}}R_T}}{2L_{\text{ST}}} \quad (2)$$

Here A_{OBS} is the observed anisotropy, Q is the ratio of the fluorescent intensities of the bound and free probe, F_{SB} is the fraction of the bound probe, A_F and A_B are the anisotropies of the free and bound probe, K_{D1} is the probe's dissociation constant, L_{ST} is the total probe concentration, and R_T is the concentration of FadD28.

Determination of dissociation rate constant of **11**-FadD28

The dissociation rate constant of **11** and FadD28 was determined by incubation of 100 nM **11** with 535 nM FadD28 in FP assay buffer ($1\times$) in a total volume of 29 μL . Next, 1 μL of tetradecanoyl-AMS **24** (100 μM final concentration) was added and FP measurements were immediately acquired in the kinetic mode and taken every 15 s until a plateau was reached. Data were fit to the one-phase exponential decay equation.

$$A_{\text{OBS}} = (A_U - A_F)10^{-k_{\text{off}}t} + A_F, \quad (3)$$

where A_U is the observed anisotropy of **11** bound to 535 nM FadD28, A_F is the anisotropy of the free probe, A_{OBS} is the observed anisotropy at time t , and k_{off} is the dissociation rate constant. All experiments were performed in duplicate.

Competitive displacement experiments

For each ligand, a threefold serial dilution series was prepared in DMSO to provide a final concentration ranging from 100 to 0.005 μM . The ligand solutions were added (1 μL in DMSO) to a FP assay mixture (29 μL) containing **11** (100 nM final concentration), FadD28 (535 nM final concentration) in FP buffer ($1\times$) in a 384-well black plate (Corning No. 3575). The plate was shaken for 5 s and read after a 10 min incubation period at 23 $^\circ\text{C}$ as described for the direct binding experiment. The K_D of each compound was determined by fitting the observed anisotropies (A_{OBS}) to Eqs. (1) and (4) by nonlinear regression analysis using Mathematica 7:

$$F_{\text{SB}} = \frac{2\sqrt{(a^2 - 3b)\cos(\theta/3)} - a}{3K_{D1} + 2\sqrt{(a^2 - 3b)\cos(\theta/3)} - a} \quad \text{with} \quad (4)$$

$$a = K_{D1} + K_{D2} + L_{\text{ST}} + L_T - R_T$$

$$b = (L_T - R_T)K_{D1} + (L_{\text{ST}} - R_T)K_{D2} + K_{D1}K_{D2}$$

$$c = -K_{D1}K_{D2}R_T$$

$$\theta = \arccos \left[\frac{-2a^3 + 9ab - 27c}{2\sqrt{(a^2 - 3b)^3}} \right]$$

Here K_{D2} is the compounds equilibrium dissociation constant, L_T is the respective concentration, and all other parameters are equivalently defined as for Eq. (2).

Isothermal titration calorimetry

ITC experiments were carried out on a Microcal VP-ITC microcalorimeter (Microcal, Inc.). All measurements were taken at 20 $^\circ\text{C}$ in 20 mM Trizma-HCl, pH 7.5, 1 mM MgCl_2 , and 0.0025% Igepal. FadD28 was dialyzed (2 L) against the buffer described above for 16 h at 4 $^\circ\text{C}$, and all ligand solutions were prepared in the final dialysate. In individual titrations, ligands were injected into the enzyme solution. Ligand and protein concentrations were 370 μM for ligand **24** and 24 μM FadD28. Titrations were carried with a stirring speed of 307 rpm and 300 s interval between 10 μL injections. The first injection was excluded from data fitting. Titrations were run past the point of enzyme saturation to determine and correct for heats of dilution. The experimental data were fit to a theoretical titration curve using the Origin software package (version 7.0) provided with the instrument to afford values of K_A (the association constant in M^{-1}), n (the number of binding sites per monomer), and ΔH (the binding enthalpy change in kilocalories per mole). The affinity of the ligand for the protein is given as the dissociation constant ($K_D = 1/K_A$). ITC experiments were performed in triplicate and analyzed independently, and the thermodynamic values obtained were averaged.

Determination of enzyme inhibition (K_i^{app})

Apparent K_i values were determined using a coupled continuous assay employing FadD28, pyrophosphatase, and nucleoside phosphorylase under initial velocity conditions as described [30]. Reactions contained 4.5 μM FadD28 in a buffer of 50 mM Trizma-HCl, pH 8.0, 2.5 mM ATP, 5 mM MgCl_2 , 0.5 mM DTT, 150 mM hydroxylamine, pH 7, 0.1 U nucleoside phosphorylase, 0.04 U pyrophosphatase, 0.2 mM 7-methylthioguanosine (MesG), and 33 μM tetradecanoic acid ($K_M = 5.3 \mu\text{M}$). Reactions were run in 96-well half-area UV Star plates (Greiner) and the cleavage of MesG was monitored at A_{360} on a Molecular Devices Spectramax M5e plate reader. K_i^{app} values were determined by fitting the concentration-response plots to the Morrison equation since the inhibitors exhibited tight-binding behavior ($K_i^{\text{app}} \leq 100 \times [E]$) [39].

$$\frac{v_i}{v_0} = 1 - \frac{([E]_T + [I]_T + K_i^{\text{app}}) - \sqrt{([E]_T + [I]_T + K_i^{\text{app}})^2 - 4[E]_T[I]_T}}{2[E]_T} \quad (5)$$

Determination of Z' and S/N for parameter optimization

FP assay mixture (29 μL) containing FadD28 (535 nM final concentration), **11** (100 nM final concentration) in FP Buffer ($1\times$) was added to 48 wells (384-well black plate) containing 1.0 μL (100 μM final volume) of tetradecanoyl-AMS **24** in DMSO to serve as a positive control and 48 wells containing 1.0 μL DMSO as the negative control. For FP signal stability studies, the plate was read at 10, 30, 60, 120, 180, and 1080 min at 23 $^\circ\text{C}$. For thermal stability studies, the plate was incubated at 23, 25, and 28 $^\circ\text{C}$ for 0.5 h and then read. The S/N and Z' values were determined from

$$S/N = \frac{A_U - A_F}{\sqrt{\sigma_U^2 + \sigma_F^2}} \quad (6)$$

$$Z' = 1 - \frac{(3\sigma_U + 3\sigma_F)}{A_U - A_F} \quad (7)$$

where A_U is the observed anisotropies in the absence of competitive ligand **24**, A_F is the observed anisotropies in the presence of 100 μM competitive ligand **24**, and σ_U and σ_F are the respective standard deviations.

High-throughput screening

The LOPAC1280 (Library of Pharmacologically Active Compounds, Sigma) library was screened for assay validation. The library was formatted into four 384-well black flat bottom plates and diluted to 1.25 mM in DMSO using a Biomek 3000 automated workstation. These plates were used to prepare screening plates in duplicate that contained 320 LOPAC compounds, 16 DMSO negative control wells (1 μ L), and 16 wells positive control wells containing **24** (1 μ L each, 100 μ M final volume) per plate. The FP assay mixture was prepared directly before the assay and contained FP buffer (30 mM Trizma-HCl, pH 7.5, 1 mM MgCl₂, 1 mM TCEP, and 0.0025% Igepal CA-630), 535 nM FadD28, and 100 nM **11**. Next, 29 μ L of the FP assay mixture was added to each well and the plates were shaken for 5 s and read after a 30 min incubation period at 23 °C as described for the direct binding experiment. The robustness of the assay was determined by calculating the Z' value for each plate using Eq. (7). The K_D's of hit compounds (Table 2) were determined against FadD28 using the competitive binding assay described above.

Results and discussion

Assay design and rationale

Our goal was to develop an assay amenable to high-throughput screening for the discovery of small molecule inhibitors of FadD28 from *M. tuberculosis*. The fluorescence polarization (FP) format was selected since it is homogeneous, allows the identification of active-site-directed inhibitors, and does not require enzyme

activity – an important consideration since the mycobacterial FadD enzymes possess low activity [31–33]. As illustrated in Fig. 3, when the fluorescent probe **11** binds to FadD28 and is excited with plane-polarized light the macromolecule complex tumbles slowly in solution and the emitted light remains largely polarized. However, when the fluorescent probe **11** is displaced by a small molecule ligand into solution, the fluorescent probe is able to rotate rapidly and consequently the emitted light is depolarized relative to the bound probe.

The most important factor in the development of an FP assay is the design of the fluorescent probe, which consists of three components: the ligand (typically active-site directed for enzyme-based assays), linker (separates the ligand from the fluorophore), and fluorophore (Fig. 4) [40]. 5'-O-[N-(Tetradecanoyl)sulfamoyl]adenosine (tetradecanoyl-AMS, **24**), a mimic of the intermediate acyl-adenylate, was selected as the ligand based on potency (vide infra) and excellent solubility (i.e., longer chain acyl groups increase potency at the expense of solubility). Ideally, the linker should be of sufficient length to enable attachment of the fluorophore without disrupting binding of the probe and also not have too many degrees of freedom, which can cause depolarization referred to as the “propeller effect” [41]. A triethyleneglycol linker was expected to provide sufficient length to access the solvent-exposed surface of the protein. Attachment of the linker at the C-2' hydroxyl was initially explored, but this modification substantially reduced binding affinity (not shown). We next, attempted to install the linker at the C-2 position of the purine and found this was tolerated as described below. When selecting an appropriate fluorophore, it is advantageous to have a fluorophore that has absorption in a range >500 nm to avoid interference by autofluorescent molecules that

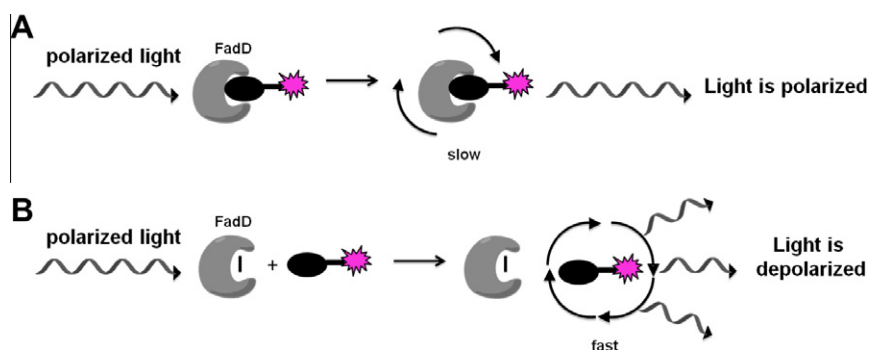


Fig. 3. Fluorescence polarization assay. General schematic for FP assay: FadD28 is represented by the gray crescent shape while the fluorescent ligand **11** is depicted as a black oval connected via a short linker to a pink fluorophore. (A) When the fluorescent probe **11** is bound to FadD28 and excited with plane-polarized light, the macromolecule complex tumbles slowly and the emitted light remains largely polarized. (B) When the fluorescent probe **11** is displaced into the bulk solution, it rotates rapidly and the emitted light is depolarized relative to the bound probe.

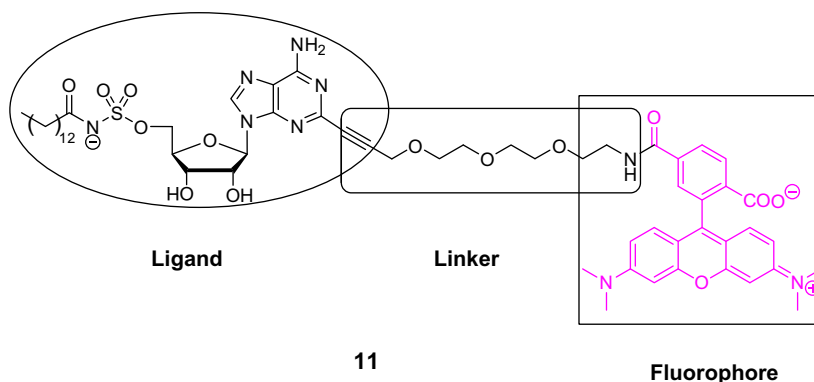
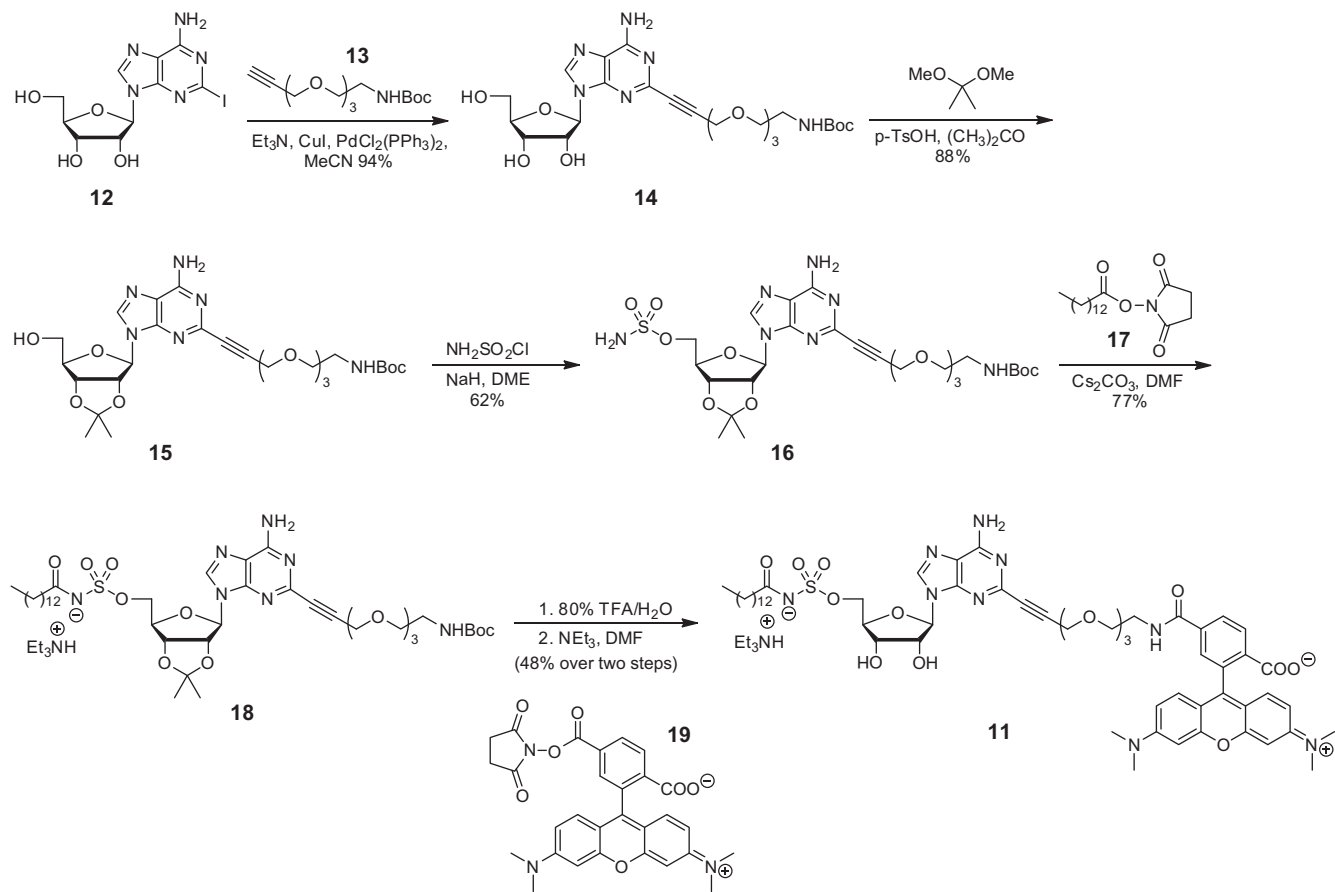


Fig. 4. Scaffold for fluorescent probe **11**.



Scheme 1.

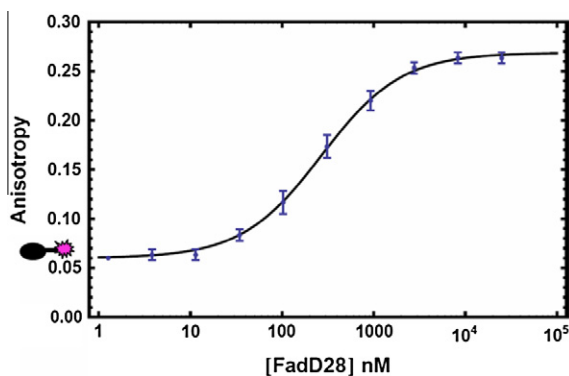


Fig. 5. Direct binding of fluorescent probe **11** (100 nM) to FadD28 as measured by fluorescence polarization. Experimental points are shown with error bars and the line is the result of fitting data to Eqs. (1) and (2).

are abundant in a high throughput libraries [42–44]. Consequently, we chose to use red shifted 5-carboxytetramethylrhodamine (TAMRA). Based on these aforementioned considerations, we designed ligand **11** (Fig. 4).

Probe synthesis

The synthesis of the fluorescent probe **11** began with the Sonogashira coupling of 2-iodoadenosine **12** [36] and alkyne linker **13** [37,38,45] to afford **14** [46] (Scheme 1). Protection of the 2'- and 3'-hydroxyls of **14** as the acetonide provided nucleoside **15**, which was sulfamoylated on the 5' position to yield **16**. Acylation with the

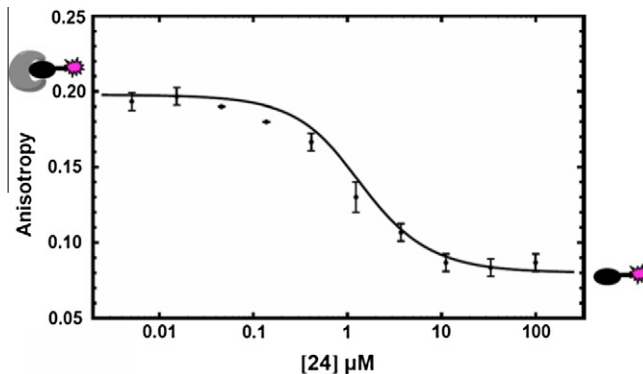


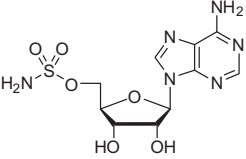
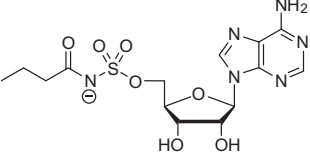
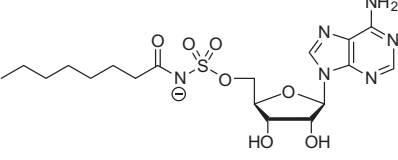
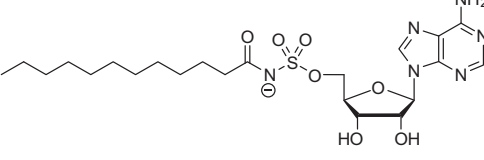
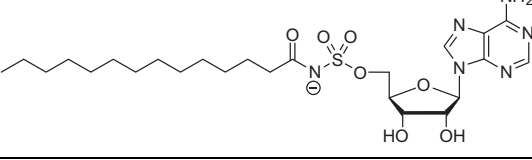
Fig. 6. Competitive displacement of fluorescent probe **11** (100 nM) from FadD28 (535 nM) with **24**. Experimental points are shown with error bars and the line is the result of fitting data to Eqs. (1) and (3).

N-hydroxysuccinidyl (NHS) ester of tetradecanoic acid **17** mediated by Cs_2CO_3 furnished acylsulfamate **18**. Deprotection of the acetonide and Boc groups of **18** was performed with an 80% aqueous TFA solution and the crude product was directly coupled with the NHS ester of 5-carboxytetramethylrhodamine **19** to provide fluorescent probe **11** as the triethylammonium salt in 19% yield over six steps.

Determination of probe K_D

Direct binding experiments were performed to determine the dissociation constant (K_D) between **11** and FadD28. Titration of

Table 1
 K_D 's and K_i^{app} 's of FadD28 inhibitors.

	Ligand	K_D (μM) ^a	K_i^{app} (μM) ^b
20		>100	nt ^c
21		>100	>100
22		1.65 ± 0.49	>100
23		0.23 ± 0.04	7.4 ± 0.6
24		0.19 ± 0.004	2.5 ± 0.2

^a K_D values were determined using the fluorescence polarization assay with 100 nM probe **11** and 535 nM FadD28.

^b K_i^{app} values were determined using the FadD28 hydroxamate–MesG coupled assay employing 33 μM tetradecanoic acid and 4.5 μM FadD28.

^c Not tested.

100 nM probe **11** with FadD28 in FP assay buffer yielded a K_D of 245 nM (Fig. 5) with a Q value of 0.91 [47]. Igepal CA-630, a non-ionic detergent, was used in the assay mixture to prevent the pronounced variation in the curvature of the meniscus in the microplate wells observed for various protein concentrations that affected fluorescent readings [48]. Additionally, non-ionic detergents reduce the potential for false positives of aggregate-based inhibitors from library screening [49–51]. The anisotropy of the unbound probe was 0.06, whereas the anisotropy of the probe bound to FadD28 was 0.25. The large anisotropy difference between the bound and free probe provides a robust signal.

Determination of K_D using FP competitive binding assay

Competitive displacement assays were performed with several ligands as a means to provide an initial level of assay validation. Roehrl et al. suggest that the fraction of the bound probe (F_{SB}) should be greater than or equal to 0.5 to ensure sufficient signal [47]. Consequently, we adjusted the concentration of the fluorescent probe **11** and FadD28 to 100 and 535 nM, respectively, to provide a $F_{SB} = 0.50$. The first ligand we examined was the parent ligand tetradecanoyl-AMS **24**, from which probe **11** was designed [30]. Titration of tetradecanoyl-AMS **24** into a solution of 100 nM **11** and 535 nM FadD28 provided a displacement curve (Fig. 6), which was analyzed as described under “Materials and Methods” to provide a K_D of 186 ± 4 nM. For direct comparison, we performed isothermal titration calorimetry (ITC) of ligand **24** with FadD28 that

yielded a K_D of 365 ± 219 nM, ΔH of -6.9 ± 0.5 kcal/mol, and n value of 1.1 ± 0.2 , indicating one substrate binding site per monomer. We also determined the apparent K_i value (K_i^{app}) of 2.5 μM for **24** with FadD28 using a coupled kinetic assay employing saturating concentrations of tetradecanoic acid (Table 1). The close agreement between the K_D 's of ligand **24** obtained by FP and ITC provides confidence in the assay. We additionally evaluated a series of ligands **20–23** (Table 1 and Fig. S1 in Supplementary data) using the competitive displacement FP assay and the coupled kinetic assay [30]. The results between both assays showed excellent correlation and K_D and K_i values both decreased with increasing chain length of the acyl moiety. The FP assay was unable to discriminate the potency of ligands **23** and **24**, since the range of resolvable inhibitor potency is limited by the affinity of the fluorescent probe [40].

Impact of control parameters

The optimization of several key factors, such as incubation time, stability of FP signal, temperature, and DMSO concentration was next assessed. In order to determine the necessary incubation time required for the assay, the dissociation rate of the probe **11** with FadD28 was measured by following the monoexponential time-dependent decrease in anisotropy following addition of a large excess of tight-binding ligand **24** (100 μM) to prebound probe **11** (100 nM) and FadD28 (535 nM). The dissociation rate-constant k_{off} is 0.0148 ± 0.0005 s⁻¹ that corresponds to a half-life of 46.9 s,

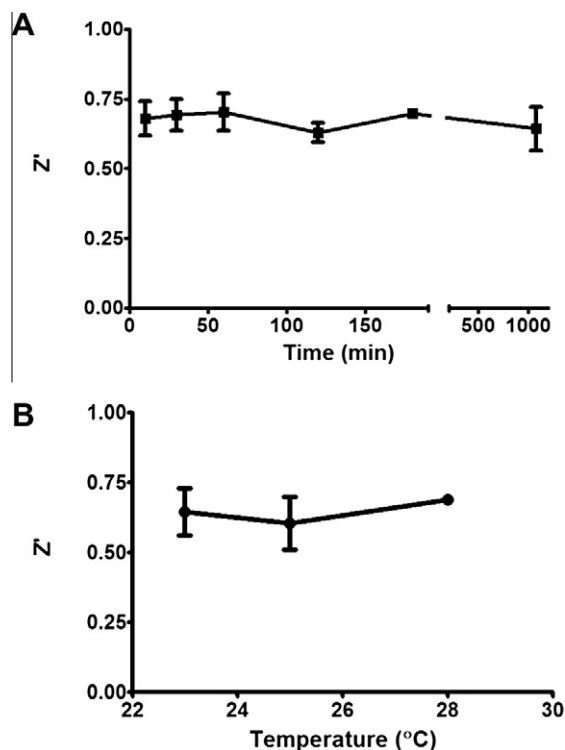


Fig. 7. Effects of incubation time (A) and temperature (B) on assay performance. Experimental points are shown with error bars.

suggesting that a 10 min incubation time is adequate. Next, the robustness of the assay was determined by evaluating the Z' value over time. Fluorescent probe **11** and FadD28 in FP buffer were incubated with **24** as a positive control or with DMSO as a negative control. The observed anisotropies were recorded at 10, 30, 60, 120, 240 and 1080 min and fit to Eq. (7) to obtain a Z' value [52]. The Z' value remained greater than 0.7 over the 24 h time period (Fig. 7A); thus the assay demonstrated excellent stability. We also showed that the signal stability as measured by Z' did not vary significantly from 23 to 28 °C (Fig. 7B). In high throughput libraries, compounds are generally dissolved in DMSO; therefore, we determined the maximum concentration of DMSO tolerated in this assay. Fluorescent probe **11** and FadD28 in FP buffer were incubated with varying concentrations of DMSO for 10 min and the observed anisotropies were recorded. From this analysis concentrations of 5% DMSO were acceptable, but the anisotropy greatly diminished at higher DMSO concentrations (data not shown); consequently, we elected to use 3% DMSO in our final assay conditions.

High-throughput screening

In order to further validate the FP assay for high throughput screening, the LOPAC1280 library was screened in duplicate against FadD28 in a 30 μ L 384-well plate format. The assay performed well with a calculated Z' factor ≥ 0.75 for each plate and a signal-to-noise >14 with four compounds exhibiting greater than 25% displacement. Z' values between 0.5 and 1.0 are considered acceptable; thus the assay was deemed suitable for high-through screening [52]. The four hit compounds were then retested using the FP competitive displacement assay to determine their respective dissociation constants (Table 2 and Fig. S2 in Supplementary data). The four compounds discovered can be grouped into two categories: ATP derivatives and long chain fatty acid derivatives. Of the ATP derivatives, 2-methylthio-ADP trisodium salt hydrate

Table 2
 K_D values of LOPAC hits.^a

Ligand	K_D (μ M) ^a
25	2.4 \pm 0.5
26	1.3 \pm 0.2
27	6.1 \pm 2.0
28	7.6 \pm 2.4

^a K_D values were determined using the fluorescence polarization assay with 100 nM probe **11** and 535 nM FadD28.

25 and 2-methylthio ATP tetrasodium **26** showed full displacement yielding K_D 's of 2.4 \pm 0.5 and 1.3 \pm 0.16 μ M, respectively (Table 2). The long chain fatty acid derivatives tetradecylthioacetic acid **27** and DL-sphinganine **28** showed only partial displacement, but the observed anisotropies could still be fit to Eqs. (1) and (4) to provide K_D 's of 6.1 \pm 2.0 and 7.6 \pm 2.4 μ M, respectively.

Conclusion

In this body of work, we have described the development of a fluorescence polarization displacement assay amenable to high-throughput screening for the discovery of active-site-directed inhibitors of FadD28 from *M. tuberculosis*. We designed and synthesized a fluorescent probe/tracer **11** that tightly binds FadD28 based on the known inhibitor **24** by attachment of the 5-carboxytetramethylrhodamine fluorophore on the C-2 position of the nucleoside moiety of **24** via a triethyleneglycol spacer. Competitive displacement experiments were performed with a series of known ligands demonstrating that the assay was robust and well-behaved. The assay was relatively insensitive to incubation time and temperature, but displayed a sharp dependence on DMSO concentration. As a final level of validation the LOPAC library was successfully screened and four ligands were identified that resulted in a greater than 25% displacement of the probe/tracer including two nucleotides and two fatty acids. These results are wholly consistent with the fatty acid–nucleoside-based FP probe/tracer **11** and demonstrate the assays readiness for high-throughput screening. We expect that the described assay can be adapted to study other FadD enzymes by suitable modification of the acyl chain to modulate binding affinity.

Acknowledgments

We thank Daniel Wilson for testing inhibitors **21–24** in the coupled kinetic assay. This research was supported by a Grant from the National Institutes of Health (NS066415).

Appendix A. Supplementary data

Supplementary data associated with this article can be found, in the online version, at doi:10.1016/j.ab.2011.06.037.

References

- [1] World Health Organization, Fact Sheet on Tuberculosis, >http://www.who.int/tb/publications/2010/factsheet_tb_2010_rev21feb11.pdf> (accessed on 16.05.11).
- [2] K. Takayama, C. Wang, G.S. Besra, Pathway to synthesis and processing of mycolic acids in *Mycobacterium tuberculosis*, Clin. Microbiol. Rev. 18 (2005) 81–101.
- [3] P.J. Brennan, H. Nikaido, The envelope of mycobacteria, Annu. Rev. Biochem. 64 (1995) 29–63.
- [4] V. Jarlier, H. Nikaido, Mycobacterial cell wall: structure and role in natural resistance to antibiotics, FEMS Microbiol. Lett. 123 (1994) 11–18.
- [5] C.E. Barry 3rd, K. Mdululi, Drug sensitivity and environmental adaptation of mycobacterial cell wall components, Trends Microbiol. 4 (1996) 275–281.
- [6] K.C. Onwueme, C.J. Vos, J. Zurita, J.A. Ferreras, L.E. Quadri, The dimycocerosate ester polyketide virulence factors of mycobacteria, Prog. Lipid Res. 44 (2005) 259–302.
- [7] M.B. Reed, P. Domenech, C. Manca, H. Su, A.K. Barczak, B.N. Kreiswirth, G. Kaplan, C.E. Barry 3rd, A glycolipid of hypervirulent tuberculosis strains that inhibits the innate immune response, Nature 431 (2004) 84–87.
- [8] M.W. Schelle, C.R. Bertozzi, Sulfate metabolism in mycobacteria, ChemBioChem 7 (2006) 1516–1524.
- [9] J.J. De Voss, K. Rutter, B.G. Schroeder, H. Su, Y. Zhu, C.E. Barry 3rd, The salicylate-derived mycobactin siderophores of *Mycobacterium tuberculosis* are essential for growth in macrophages, Proc. Natl. Acad. Sci. USA 97 (2000) 1252–1257.
- [10] J.D. McKinney, K. Honer zu Bentrup, E.J. Munoz-Elias, A. Miczak, B. Chen, W.T. Chan, D. Swenson, J.C. Sacchetti, W.R. Jacobs Jr., D.G. Russell, Persistence of *Mycobacterium tuberculosis* in macrophages and mice requires the glyoxylate shunt enzyme isocitrate lyase, Nature 406 (2000) 735–738.
- [11] J. Timm, F.A. Post, L.G. Bekker, G.B. Walthers, H.C. Wainwright, R. Manganelli, W.T. Chan, L. Tsenova, B. Gold, I. Smith, G. Kaplan, J.D. McKinney, Differential expression of iron-, carbon-, and oxygen-responsive mycobacterial genes in the lungs of chronically infected mice and tuberculosis patients, Proc. Natl. Acad. Sci. USA 100 (2003) 14321–14326.
- [12] O.A. Trivedi, P. Arora, V. Sridharan, R. Tickoo, D. Mohanty, R.S. Gokhale, Enzymic activation and transfer of fatty acids as acyl-adenylates in mycobacteria, Nature 428 (2004) 441–445.
- [13] S.T. Cole, R. Brosch, J. Parkhill, T. Garnier, C. Churcher, D. Harris, S.V. Gordon, K. Eiglmeier, S. Gas, C.E. Barry 3rd, F. Tekaiia, K. Badcock, D. Basham, D. Brown, T. Chillingworth, R. Connor, R. Davies, K. Devlin, T. Feltwell, S. Gentles, N. Hamlin, S. Holroyd, T. Hornsby, K. Jagels, A. Krogh, J. McLean, S. Moule, L. Murphy, K. Oliver, J. Osborne, M.A. Quail, M.A. Rajandream, J. Rogers, S. Rutter, K. Seeger, J. Skelton, R. Squares, S. Squares, J.E. Sulston, K. Taylor, S. Whitehead, B.G. Barrell, Deciphering the biology of *Mycobacterium tuberculosis* from the complete genome sequence, Nature 393 (1998) 537–544.
- [14] P. Arora, A. Goyal, V.T. Natarajan, E. Rajakumara, P. Verma, R. Gupta, M. Yousuf, O.A. Trivedi, D. Mohanty, A. Tyagi, R. Sankaranarayanan, R.S. Gokhale, Mechanistic and functional insights into fatty acid activation in *Mycobacterium tuberculosis*, Nat. Chem. Biol. 5 (2009) 166–173.
- [15] P. Arora, A. Vats, P. Saxena, D. Mohanty, R.S. Gokhale, Promiscuous fatty acyl CoA ligases produce acyl-CoA and acyl-SNAC precursors for polyketide biosynthesis, J. Am. Chem. Soc. 127 (2005) 9388–9389.
- [16] G. Khare, V. Gupta, R.K. Gupta, R. Gupta, R. Bhat, A.K. Tyagi, Dissecting the role of critical residues and substrate preference of a fatty acyl-CoA synthetase (FadD13) of *Mycobacterium tuberculosis*, PLoS One 4 (2009) e8387.
- [17] C.M. Sasseti, D.H. Boyd, E.J. Rubin, Genes required for mycobacterial growth defined by high density mutagenesis, Mol. Microbiol. 48 (2003) 77–84.
- [18] R.S. Gokhale, P. Saxena, T. Chopra, D. Mohanty, Versatile polyketide enzymatic machinery for the biosynthesis of complex mycobacterial lipids, Nat. Prod. Rep. 24 (2007) 267–277.
- [19] D. Portevin, C. de Sousa-D'Auria, H. Montrozier, C. Houssin, A. Stella, M.A. Laneelle, F. Bardou, C. Guilhot, M. Daffe, The acyl-AMP ligase FadD32 and AccD4-containing acyl-CoA carboxylase are required for the synthesis of mycolic acids and essential for mycobacterial growth: identification of the carboxylation product and determination of the acyl-CoA carboxylase components, J. Biol. Chem. 280 (2005) 8862–8874.
- [20] S. Gavalda, M. Leger, B. van der Rest, A. Stella, F. Bardou, H. Montrozier, C. Chalut, O. Burlet-Schiltz, H. Marrakchi, M. Daffe, A. Quemard, The Pks13/FadD32 crosstalk for the biosynthesis of mycolic acids in *Mycobacterium tuberculosis*, J. Biol. Chem. 284 (2009) 19255–19264.
- [21] M. Leger, S. Gavalda, V. Guillet, B. van der Rest, N. Slama, H. Montrozier, L. Mourey, A. Quemard, M. Daffe, H. Marrakchi, The dual function of the *Mycobacterium tuberculosis* FadD32 required for mycolic acid biosynthesis, Chem. Biol. 16 (2009) 510–519.
- [22] L. Rindi, L. Fattorini, D. Bonanni, E. Iona, G. Freer, D. Tan, G. Deho, G. Orefici, C. Garzelli, Involvement of the *fadD33* gene in the growth of *Mycobacterium tuberculosis* in the liver of BALB/c mice, Microbiology 148 (2002) 3873–3880.
- [23] L. Rindi, D. Bonanni, N. Lari, C. Garzelli, Requirement of gene *fadD33* for the growth of *Mycobacterium tuberculosis* in a hepatocyte cell line, New Microbiol. 27 (2004) 125–131.
- [24] R. Kritchika, U. Marathe, P. Saxena, M.Z. Ansari, D. Mohanty, R.S. Gokhale, A genetic locus required for iron acquisition in *Mycobacterium tuberculosis*, Proc. Natl. Acad. Sci. USA 103 (2006) 2069–2074.
- [25] T.D. Sirakova, A.M. Fitzmaurice, P. Kolattukudy, Regulation of expression of *mas* and *fadD28*, two genes involved in production of dimycocerosyl phthiocerol, a virulence factor of *Mycobacterium tuberculosis*, J. Bacteriol. 184 (2002) 6796–6802.
- [26] O.A. Trivedi, P. Arora, A. Vats, M.Z. Ansari, R. Tickoo, V. Sridharan, D. Mohanty, R.S. Gokhale, Dissecting the mechanism and assembly of a complex virulence mycobacterial lipid, Mol. Cell 17 (2005) 631–643.
- [27] R. Simeone, M. Leger, P. Constant, W. Malaga, H. Marrakchi, M. Daffe, C. Guilhot, C. Chalut, Delineation of the roles of FadD22, FadD26 and FadD29 in the biosynthesis of phthiocerol dimycocerosates and related compounds in *Mycobacterium tuberculosis*, FEBS J. 277 (2010) 2715–2725.
- [28] J.A. Ferreras, K.L. Stirrett, X. Lu, J.S. Ryu, C.E. Soll, D.S. Tan, L.E. Quadri, Mycobacterial phenolic glycolipid virulence factor biosynthesis: mechanism and small-molecule inhibition of polyketide chain initiation, Chem. Biol. 15 (2008) 51–61.
- [29] J. Lynett, R.W. Stokes, Selection of transposon mutants of *Mycobacterium tuberculosis* with increased macrophage infectivity identifies *fadD23* to be involved in sulfolipid production and association with macrophages, Microbiology 153 (2007) 3133–3140.
- [30] D.J. Wilson, C.C. Aldrich, A continuous kinetic assay for adenylation enzyme activity and inhibition, Anal. Biochem. 404 (2010) 56–63.
- [31] T.J. Burke, K.R. Loniello, J.A. Beebe, K.M. Ervin, Development and application of fluorescence polarization assays in drug discovery, Comb. Chem. High Throughput Screen. 6 (2003) 183–194.
- [32] M. Hafner, E. Vianini, B. Albertoni, L. Marchetti, I. Grune, C. Gloeckner, M. Famulok, Displacement of protein-bound aptamers with small molecules screened by fluorescence polarization, Nat. Protoc. 3 (2008) 579–587.
- [33] M.H. Roehrl, J.Y. Wang, G. Wagner, A general framework for development and data analysis of competitive high-throughput screens for small-molecule inhibitors of protein-protein interactions by fluorescence polarization, Biochemistry 43 (2004) 16056–16066.
- [34] A. Goyal, M. Yousuf, E. Rajakumara, P. Arora, R.S. Gokhale, R. Sankaranarayanan, Crystallization and preliminary X-ray crystallographic studies of the N-terminal domain of FadD28, a fatty-acyl AMP ligase from *Mycobacterium tuberculosis*, Acta Crystallogr. Sect. F: Struct. Biol. Cryst. Commun. 62 (2006) 350–352.
- [35] D. Heacock, C.J. Forsyth, K. Shiba, K. Musier-Forsyth, Synthesis and aminoacyl-tRNA synthetase inhibitory activity of prolyl adenylate analogs, Bioorg. Chem. 24 (1996) 273–289.
- [36] A. Matsuda, M. Shinozaki, T. Yamaguchi, H. Homma, R. Nomoto, T. Miyasaka, Y. Watanabe, T. Abiru, Nucleosides and nucleotides. 103. 2-Alkynyladenosines: a novel class of selective adenosine A2 receptor agonists with potent antihypertensive effects, J. Med. Chem. 35 (1992) 241–252.
- [37] E. Fernandez-Megia, J. Correa, I. Rodriguez-Meizoso, R. Riguera, A click approach to unprotected glycodendrimers, Macromolecules 39 (2006) 2113–2120.
- [38] L. Lebeau, P. Oudet, C. Mioskowski, Synthesis of new phospholipids linked to steroid-hormone derivatives designed for two-dimensional crystallization of proteins, Helv. Chim. Acta 74 (1991) 1697–1706.
- [39] R.A. Copeland, Tight Binding Inhibitors. Evaluation of Enzyme Inhibitors in Drug Discovery, Wiley, Hoboken, NJ, 2005, pp. 185–187.
- [40] X. Huang, Fluorescence polarization competition assay: the range of resolvable inhibitor potency is limited by the affinity of the fluorescent ligand, J. Biomol. Screen. 8 (2003) 34–38.
- [41] B.A. Lynch, K.A. Loiacono, C.L. Tiong, S.E. Adams, I.A. MacNeil, A fluorescence polarization based Src-SH2 binding assay, Anal. Biochem. 247 (1997) 77–82.
- [42] K.L. Vedvik, H.C. Eliason, R.L. Hoffman, J.R. Gibson, K.R. Kupcho, R.L. Somberg, K.W. Vogel, Overcoming compound interference in fluorescence polarization-based kinase assays using far-red tracers, Assay Drug. Dev. Technol. 2 (2004) 193–203.
- [43] G.R. Nakayama, P. Bingham, D. Tan, K.A. Maegley, A fluorescence polarization assay for screening inhibitors against the ribonuclease H activity of HIV-1 reverse transcriptase, Anal. Biochem. 351 (2006) 260–265.
- [44] A. Vaasa, I. Viil, E. Enkvist, K. Viht, G. Raidaru, D. Lavogina, A. Uri, High-affinity bisubstrate probe for fluorescence anisotropy binding/displacement assays with protein kinases PKA and ROCK, Anal. Biochem. 385 (2009) 85–93.
- [45] E.W. van Tilburg, M. Gremmen, J. von Frijtag Drabbe Kunzel, M. de Groot, A.P. IJzerman, 2, 8-Disubstituted adenosine derivatives as partial agonists for the adenosine A2A receptor, Bioorg. Med. Chem. 11 (2003) 2183–2192.
- [46] F. Guo, S. Das, B.M. Mueller, C.F. Barbas 3rd, R.A. Lerner, S.C. Sinha, Breaking the one antibody-one target axiom, Proc. Natl. Acad. Sci. USA 103 (2006) 11009–11014.
- [47] M.H. Roehrl, J.Y. Wang, G. Wagner, Discovery of small-molecule inhibitors of the NFAT-calcineurin interaction by competitive high-throughput fluorescence polarization screening, Biochemistry 43 (2004) 16067–16075.
- [48] J. Neres, D.J. Wilson, L. Celia, B.J. Beck, C.C. Aldrich, Aryl acid adenylation enzymes involved in siderophore biosynthesis: fluorescence polarization assay, ligand specificity, and discovery of non-nucleoside inhibitors via high-throughput screening, Biochemistry 47 (2008) 11735–11749.
- [49] S.L. McGovern, B.T. Helfand, B. Feng, B.K. Shoichet, A specific mechanism of nonspecific inhibition, J. Med. Chem. 46 (2003) 4265–4272.
- [50] B.Y. Feng, B.K. Shoichet, A detergent-based assay for the detection of promiscuous inhibitors, Nat. Protoc. 1 (2006) 550–553.
- [51] B.Y. Feng, A. Simeonov, A. Jadhav, K. Babaoglu, J. Ingles, B.K. Shoichet, C.P. Austin, A high-throughput screen for aggregation-based inhibition in a large compound library, J. Med. Chem. 50 (2007) 2385–2390.
- [52] J.H. Zhang, T.D. Chung, K.R. Oldenburg, A simple statistical parameter for use in evaluation and validation of high throughput screening assays, J. Biomol. Screen. 4 (1999) 67–73.